The Astrophysical Journal Letters, 833:L5 (7pp), 2016 December 10 doi:10.3847/2041-8205/833/1/L5

AN ULTRA-FAINT GALAXY CANDIDATE DISCOVERED IN EARLY DATA FROM THE MAGELLANIC SATELLITES SURVEY

A. Drlica-Wagner[1], K. Bechtol[2,3], S. Allam[1], D. L. Tucker[1], R. A. Gruendl[4,5], M. D. Johnson[5], A. R. Walker[6], D. J. James[6], D. L. Nidever[7], K. A. G. Olsen[7], R. H. Wechsler[8,9,10], M. R. L. Cioni[11,12,13], B. C. Conn[14], K. Kuehn[15], T. S. Li[1], Y.-Y. Mao[16,17], N. F. Martin[18,19], E. Neilsen[1], N. E. D. Noel[20], A. Pieres[21,22], J. D. Simon[23], G. S. Stringfellow[24], R. P. van der Marel[25], and B. Yanny[1]

[1] Fermi National Accelerator Laboratory, P.O. Box 500, Batavia, IL 60510, USA; kadrlica@fnal.gov
[2] Wisconsin IceCube Particle Astrophysics Center (WIPAC), Madison, WI 53703, USA; keith.bechtol@icecube.wisc.edu
[3] Department of Physics, University of Wisconsin–Madison, Madison, WI 53706, USA
[4] Department of Astronomy, University of Illinois, 1002 W. Green Street, Urbana, IL 61801, USA
[5] National Center for Supercomputing Applications, 1205 West Clark Street, Urbana, IL 61801, USA
[6] Cerro Tololo Inter-American Observatory, National Optical Astronomy Observatory, Casilla 603, La Serena, Chile
[7] National Optical Astronomy Observatory, 950 N. Cherry Avenue, Tucson, AZ 85719, USA
[8] Department of Physics, Stanford University, 382 Via Pueblo Mall, Stanford, CA 94305, USA
[9] Kavli Institute for Particle Astrophysics & Cosmology, P.O. Box 2450, Stanford University, Stanford, CA 94305, USA
[10] SLAC National Accelerator Laboratory, Menlo Park, CA 94025, USA
[11] Universität Potsdam, Institut für Physik und Astronomie, Karl-Liebknecht-Str. 24/25, D-14476 Potsdam, Germany
[12] Leibnitz-Institut für Astrophysik Potsdam, An der Sternwarte 16, D-14482 Potsdam, Germany
[13] University of Hertfordshire, Physics Astronomy and Mathematics, College Lane, Hatfield AL10 9AB, UK
[14] Research School of Astronomy & Astrophysics, Mount Stromlo Observatory, Cotter Road, Weston Creek, ACT 2611, Australia
[15] Australian Astronomical Observatory, North Ryde, NSW 2113, Australia
[16] Department of Physics and Astronomy, University of Pittsburgh, Pittsburgh, PA 15260, USA
[17] Pittsburgh Particle Physics, Astrophysics, and Cosmology Center (PITT PACC), University of Pittsburgh, Pittsburgh, PA 15260, USA
[18] Observatoire astronomique de Strasbourg, Université de Strasbourg, CNRS, UMR 7550, 11 rue de l'Université, F-67000 Strasbourg, France
[19] Max-Planck-Institut für Astronomie, Königstuhl 17, D-69117 Heidelberg, Germany
[20] Department of Physics, University of Surrey, Guildford GU2 7XH, UK
[21] Instituto de Física, UFRGS, Caixa Postal 15051, Porto Alegre, RS—91501-970, Brazil
[22] Laboratório Interinstitucional de e-Astronomia—LIneA, Rua Gal. José Cristino 77, Rio de Janeiro, RJ—20921-400, Brazil
[23] Carnegie Observatories, 813 Santa Barbara St., Pasadena, CA 91101, USA
[24] Center for Astrophysics and Space Astronomy, University of Colorado, 389 UCB, Boulder, CO 80309-0389, USA
[25] Space Telescope Science Institute, 3700 San Martin Drive, Baltimore, MD 21218, USA
Received 2016 September 6; revised 2016 October 23; accepted 2016 October 24; published 2016 November 30

ABSTRACT

We report a new ultra-faint stellar system found in Dark Energy Camera data from the first observing run of the Magellanic Satellites Survey (MagLiteS). MagLiteS J0644−5953 (Pictor II or Pic II) is a low surface brightness ($\mu = 28.5^{+1}_{-1}$ mag arcsec $^{-2}$ within its half-light radius) resolved overdensity of old and metal-poor stars located at a heliocentric distance of 45^{+5}_{-4} kpc. The physical size ($r_{1/2} = 46^{+15}_{-11}$ pc) and low luminosity ($M_V = -3.2^{+0.4}_{-0.5}$ mag) of this satellite are consistent with the locus of spectroscopically confirmed ultra-faint galaxies. MagLiteS J0644−5953 (Pic II) is located $11.3^{+3.1}_{-0.9}$ kpc from the Large Magellanic Cloud (LMC), and comparisons with simulation results in the literature suggest that this satellite was likely accreted with the LMC. The close proximity of MagLiteS J0644−5953 (Pic II) to the LMC also makes it the most likely ultra-faint galaxy candidate to still be gravitationally bound to the LMC.

Key words: galaxies: dwarf – Local Group – Magellanic Clouds

1. INTRODUCTION

The standard cosmological model generically predicts the formation of structure over a wide range of mass scales from galaxy clusters to ultra-faint galaxies. The Local Group offers a unique environment to search for evidence of hierarchical structure formation on the smallest scales.

For decades authors have speculated that some of the smaller Milky Way satellites may have originated with the Large and Small Magellanic Clouds (LMC, SMC; e.g., Lynden-Bell 1976; D'Onghia & Lake 2008; Nichols et al. 2011; Sales et al. 2011). The recent discovery of more than 20 ultra-faint ($M_V \gtrsim -8$) galaxy candidates by wide-area optical surveys, including the Dark Energy Survey (DES; Bechtol et al. 2015; Drlica-Wagner et al. 2015; Kim & Jerjen 2015; Koposov et al. 2015a), the Survey of the MAgellanic Stellar History (SMASH; Martin et al. 2015), Pan-STARRS (Laevens et al. 2015a, 2015b), and VST ATLAS (Torrealba et al. 2016a, 2016b), has renewed interest in identifying faint galactic companions of the Magellanic Clouds. Indeed, 15 of the 17 candidates in the DES footprint are located in the southern half of the surveyed area, near the Magellanic Clouds. This inhomogeneity in the spatial distribution of satellites allows the DES data alone to exclude an isotropic spatial distribution of Milky Way satellites at the 3σ level (Drlica-Wagner et al. 2015). Instead, the observed distribution can be well, though not uniquely, described by an association between several of the new satellites and the Magellanic system. Simple models incorporating DES and SDSS observations predict that the entire sky may contain ∼100 ultra-faint galaxies with physical properties comparable to the DES satellites and that 20%–30% of these could be spatially associated with the Magellanic Clouds (Drlica-Wagner et al. 2015).

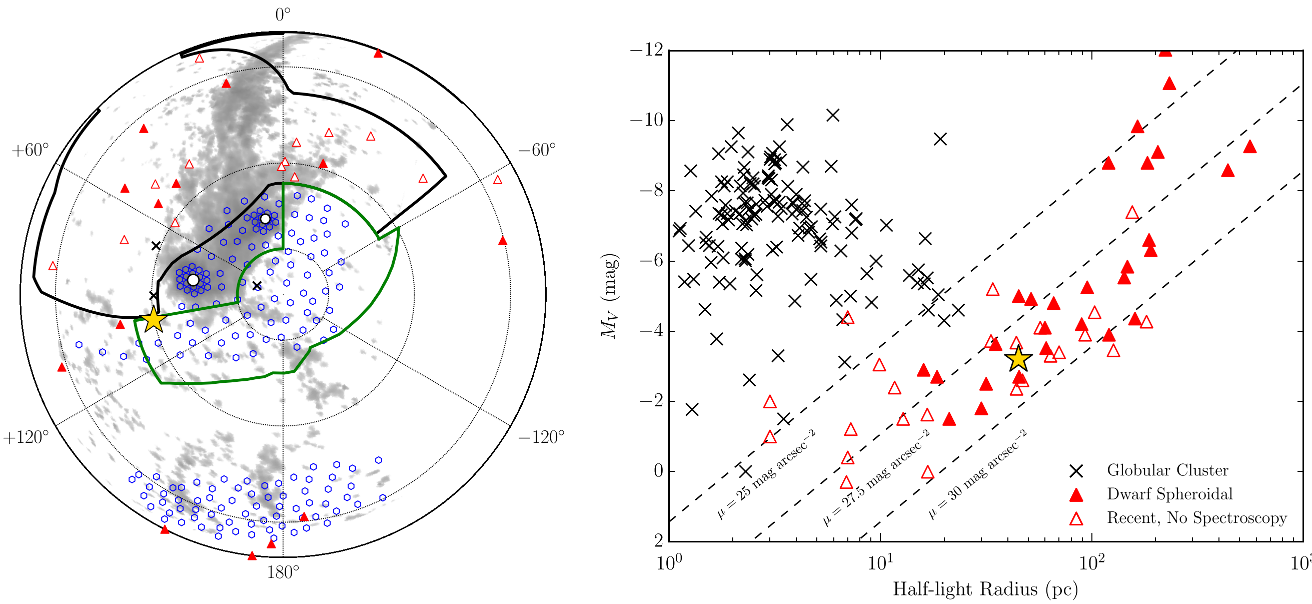

Figure 1. Left: orthonormal projection of the southern celestial hemisphere showing the H I density of the Magellanic Stream in grayscale (Nidever et al. 2010). Overplotted are the footprints of DES (black), MagLiteS (green), and SMASH (blue hexagons representing individual DECam pointings). The location of MagLiteS J0644−5953 (Pic II) is shown with a gold star. Other candidate and confirmed Milky Way satellite galaxies are marked with triangles. The distant LMC star clusters NGC 1841, Reticulum, and ESO 121-SC03 are marked with black crosses. Right: absolute visual magnitude (M_V) vs. azimuthally averaged physical half-light radius ($r_{1/2}$) for dwarf galaxies (solid red triangles), globular clusters (black crosses), and recently discovered systems lacking spectroscopic measurements (open red triangles). The black dashed lines indicate contours of constant surface brightness (μ; average within the half-light radius). MagLiteS J0644−5953 (Pic II) is marked by a gold star.

These conclusions are largely supported by detailed simulations (Deason et al. 2015; Wheeler et al. 2015; Yozin & Bekki 2015; Jethwa et al. 2016; Sales et al. 2016), which also find evidence for a Magellanic bias in the Milky Way satellite distribution. In addition, the systemic radial velocities of several of the newly discovered satellites may be consistent with the orbit of the Clouds (Koposov et al. 2015b; Jethwa et al. 2016; Sales et al. 2016; Walker et al. 2016).

Since the Magellanic Clouds are likely on their first passage around the Milky Way (Besla et al. 2007; Busha et al. 2011; Kallivayalil et al. 2013), satellite galaxies that originated with the Clouds would have formed in an environment that was rather different from the one they inhabit today. Comparing these systems to systems that formed around the Milky Way or far from any massive host would test environmental influences on the age, star formation history, and chemical evolution of the smallest galaxies. Furthermore, the existence and properties of satellites of satellites can test the hierarchical structure predictions of ΛCDM.

Two low-luminosity satellites have been recently found around more isolated Local Volume analogs of the Magellanic Clouds: Antlia B around NGC 3109 (Sand et al. 2015) and MADCASH J074238+652501-dw around NGC 2403 (Carlin et al. 2016). Satellite-host associations are more certain in these cases relative to the Magellanic system, due to the absence of a nearby large galaxy like the Milky Way. However, only the Magellanic Clouds are close enough to efficiently detect and characterize ultra-faint satellites.

The Magellanic SatelLites Survey (MagLiteS; PI: K. Bechtol) is a National Optical Astronomy Observatory (NOAO) community survey that uses the Dark Energy Camera (DECam; Flaugher et al. 2015) to complete an annulus of contiguous imaging around the periphery of the Magellanic system (Figure 1). In Section 2 we describe the scope and progress of MagLiteS. Initial inspection of stellar catalogs assembled from the first MagLiteS observing run (R1) revealed a resolved stellar overdensity at $(\alpha_{2000}, \delta_{2000}) = (101\overset{\circ}{.}180, -59\overset{\circ}{.}897)$, as described in Section 3. The physical properties of this satellite are similar to known ultra-faint galaxies (Figure 1, right panel), and are detailed in Section 4. In Section 5 we conclude by discussing the possible association between this stellar system and the Magellanic Clouds.

This satellite resides in the constellation Pictor, and if it is confirmed to be a dark-matter-dominated galaxy, it would be named Pictor II (Pic II); otherwise it will be named MagLiteS 1. Until spectroscopic observations clarify the physical nature of this system, we refer to it as (Pic II).

2. MAGLITES DATA

MagLiteS is an ongoing optical imaging survey using DECam on the 4 m Blanco Telescope at the Cerro Tololo Inter-American Observatory to map ∼1200 deg^2 near the south celestial pole (Figure 1). MagLiteS relies on the large field of view of DECam (∼3 deg^2) to cover this area in 12 nights distributed over the 2016A and 2017A semesters. During this period the survey footprint will be covered with three dithered tilings. Each tiling consists of one 90 s exposure in the DES g-band and a co-located 90 s exposure in the DES r-band such that color–magnitude diagrams can be generated. The median 10σ limiting depth of MagLiteS is $\gtrsim$23 mag in both bands, which is roughly comparable to the first two years of imaging by DES (Drlica-Wagner et al. 2015).

The first observing run (R1) of MagLiteS took place over six half-nights between 2016 February 10 and 15. Observing conditions were variable, with seeing between 0$\overset{\prime\prime}{.}$8 and 1$\overset{\prime\prime}{.}$5. MagLiteS R1 consists of 725 survey exposures collected over an area of ∼600 deg^2 (∼20% of the exposures were in the second tiling). Due to the southern latitude of the MagLiteS footprint, the airmass (and accordingly the point-spread function) of the MagLiteS exposures is higher than that of the DES exposures.

The MagLiteS exposures were reduced and processed by the DES Data Management system using the same pipeline developed for the year-three annual reprocessing of the DES data (see Sevilla et al. 2011; Mohr et al. 2012, for an overview of the processing pipeline). Astronomical source detection and photometry were performed on a per exposure basis using the `PSFex` and `SExtractor` routines (Bertin & Arnouts 1996; Bertin 2011). As part of this step, astrometric calibration was performed with `SCAMP` (Bertin 2006) by matching objects to the UCAC-4 catalog (Zacharias et al. 2013). The `SExtractor` source detection threshold was set to detect sources with $S/N \gtrsim 5$. Photometric fluxes and magnitudes refer to the `SExtractor` PSF model fit.

Unique object catalogs were assembled by performing a $1''$ match on objects detected in individual exposures. During the catalog generation process, we flagged problematic images (e.g., CCDs suffering from reflected light, imaging artifacts, point-spread function misestimation, etc.) and excluded the affected objects from subsequent analyses. Stellar objects were selected based on the *spread_model* quantity: $|wavg\_spread\_model\_r| < 0.003 + spreaderr\_model\_r$ (e.g., Drlica-Wagner et al. 2015).

Photometric calibration was performed by matching stars to the APASS catalog on a CCD-by-CCD basis. APASS-measured magnitudes were transformed to the DES system before calibration:

$$g_{\rm DES} = g_{\rm APASS} - 0.0642(g_{\rm APASS} - r_{\rm APASS}) - 0.0239$$
$$r_{\rm DES} = r_{\rm APASS} - 0.1264(r_{\rm APASS} - i_{\rm APASS}) - 0.0098.$$

For a small number of CCDs where too few stars were matched, or the resulting zeropoint was a strong outlier with respect to the other CCDs in that exposure, zeropoints were instead derived from a simultaneous fit to all CCDs on the exposure. The zeropoints derived from APASS were found to agree well with a set of zeropoint solutions derived by the photometric standards module (Tucker et al. 2007) on four photometric nights. Extinction from interstellar dust was calculated for each object from a bilinear interpolation of the extinction maps of Schlegel et al. (1998). We followed the procedure of Schlafly & Finkbeiner (2011) to calculate reddening, assuming $R_V = 3.1$; however, in contrast to Schlafly & Finkbeiner (2011), we used a set of $A_b/E(B - V)$ coefficients derived by DES for the g and r bands: $A_g/E(B - V) = 3.683$ and $A_r/E(B - V) = 2.605$. All magnitudes quoted in the remainder of this letter have been dereddened using this procedure.

3. SATELLITE SEARCH

We performed a search for arcminute-scale stellar overdensities following the maximum-likelihood procedure described in Bechtol et al. (2015).[26] Specifically, we scanned the MagLiteS R1 data testing for the presence of a satellite galaxy at each location on a multi-dimensional grid of sky position ($0\farcm7$ resolution; `HEALPix` *nside* = 4096) and distance modulus ($16\ {\rm mag} < m - M < 23\ {\rm mag}$). Our spatial model assumed a radially symmetric Plummer kernel with half-light radius of $r_h = 4'$. The satellite template in color–magnitude space consisted of four `PARSEC` isochrones (Bressan et al. 2012) with $\tau = \{10\ {\rm Gyr}, 12\ {\rm Gyr}\}$ and $Z = \{0.0001, 0.0002\}$ each weighted by a Chabrier (2001) initial mass function.

As noted in Section 2, the MagLiteS R1 data predominantly consists of a single DECam tiling. This leads to a complicated coverage pattern including gaps between CCDs, regions of significantly decreased depth due to cloudy conditions, and holes caused by scattered light from bright stars. The maximum-likelihood analysis is capable of accounting for inhomogeneities in survey coverage, as long as they are well-characterized by a survey coverage mask. However, inconsistencies between the parameterized coverage mask and the true survey coverage can lead to spurious detections. While these artifacts are easily identified from visual inspection of their morphological and photometric properties, their prevalence made a systematic search of the early MagLiteS data difficult. We expect these issues to be mitigated by increased survey uniformity from upcoming observations. Here, we focus on the fortuitous discovery of a previously unidentified stellar overdensity, MagLiteS J0644−5953 (Pic II), which was identified by the likelihood search and passed all visual inspection tests (Figure 2). This system was identified with a likelihood ratio test statistic TS = 235, which corresponds to a Gaussian significance of $\sim 15\sigma$.

4. PROPERTIES OF MAGLITES J0644–5953 (PIC II)

We simultaneously fit the morphological and isochrone parameters of MagLiteS J0644−5953 (Pic II) with the same maximum-likelihood approach used for our search. We performed a nine-parameter fit of stellar richness (λ), centroid position (α_{2000},δ_{2000}), semimajor half-light radius (a_h), ellipticity (ϵ), position angle (P.A.), distance modulus ($m - M$), age (τ), and metallicity (Z) of the stellar population. We explored this multi-dimensional parameter space with $\sim 8 \times 10^5$ samples from an affine invariant Markov Chain Monte Carlo (MCMC) ensemble sampler (Foreman-Mackey et al. 2013).[27] We imposed a Jeffreys' prior on the extension, $\mathcal{P}(a_h) \propto 1/a_h$, and flat priors on all other parameters. During the fit, we used a single `PARSEC` isochrone with age and metallicity varying between $1\ {\rm Gyr} < \tau < 13.5\ {\rm Gyr}$ and $0.0001 < Z < 0.01$, respectively. Masking a bright star $4\farcm4$ southeast of MagLiteS J0644−5953 (Pic II) may bias the fit at the 1% level.

The resulting posterior probability distributions are shown in Figure 3. Best-fit parameters were derived from the peak of the posterior probability distribution as determined by a kernel density estimate, while uncertainties were derived from the maximum density interval that encloses 90% of the posterior density. The absolute V-band magnitude was calculated according to the prescription of Martin et al. (2008) and does not include the uncertainty on distance. The properties of MagLiteS J0644−5953 (Pic II) are collected in Table 1.

Like the other parameters shown in Table 1, the distance modulus of MagLiteS J0644−5953 (Pic II) was derived from a simultaneous likelihood fit to the CMD and spatial information. The best-fit distance modulus was driven by the position of the main sequence turnoff and was only moderately influenced by potential member stars in the horizontal branch. The statistical

[26] https://github.com/DarkEnergySurvey/ugali

[27] `emcee` v2.2.0: http://dan.iel.fm/emcee/.

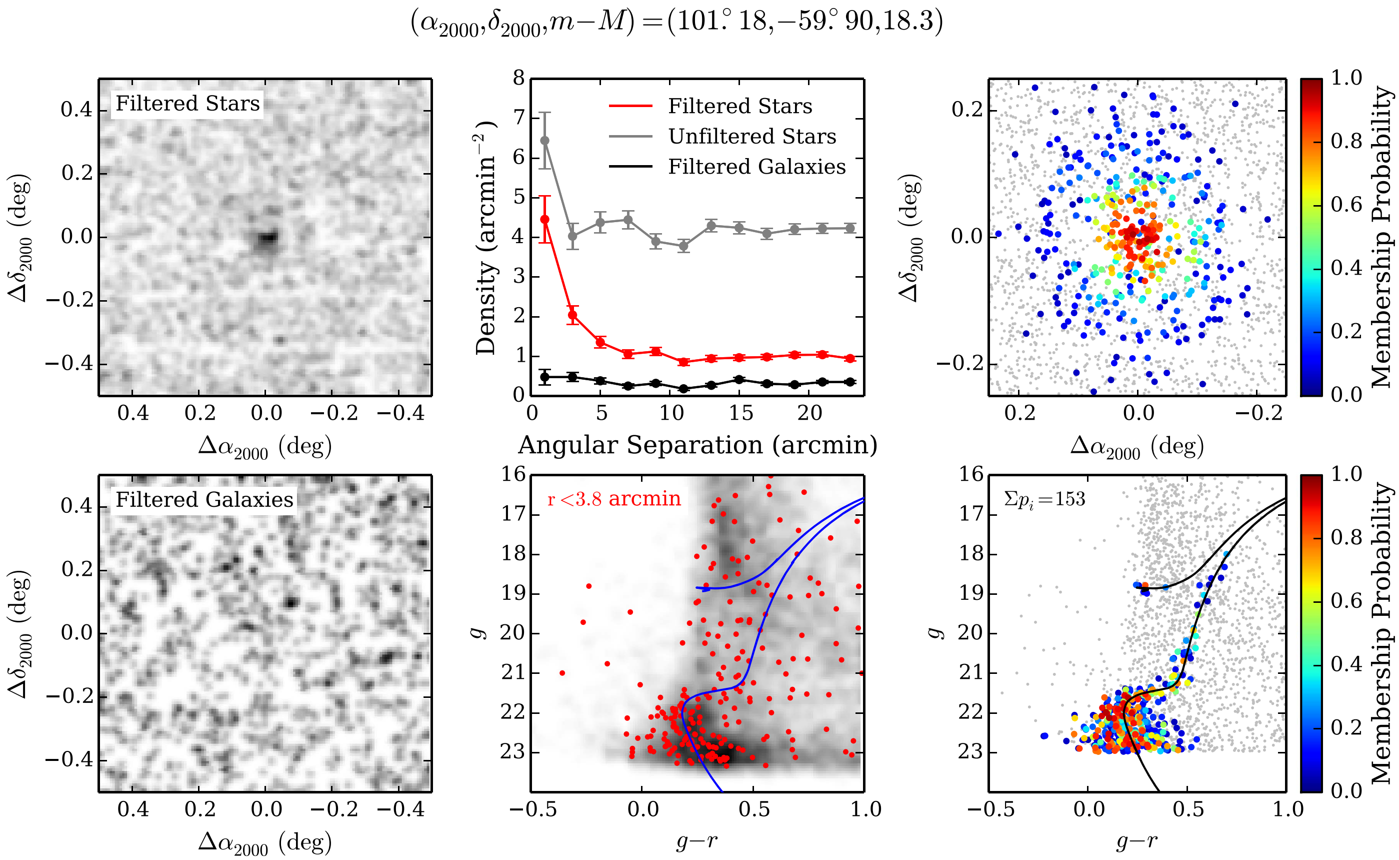

Figure 2. Stellar density and color–magnitude diagrams for (Pic II). Top left: spatial distribution of stars with $g < 24$ mag that pass the isochrone filter (see the text). The field of view is $1^\circ \times 1^\circ$ centered on the candidate and the stellar distribution has been smoothed by a Gaussian kernel with standard deviation $0\farcm6$. Top center: radial distribution of objects with $g - r < 1$ mag and $g < 24$ mag : stars passing the isochrone filter (red), stars excluded from the isochrone filter (gray), and galaxies passing the isochrone filter (black). Top right: spatial distribution of stars with high membership probabilities within a $0\fdg5 \times 0\fdg5$ field of view. Gray points indicate stars with a membership probability less than 5%. Bottom left: same as the top left panel, but for galaxies passing the isochrone filter. Bottom center: the color–magnitude distribution of stars within $r = 3\farcm8$ of the centroid are indicated with individual points. The density of the field within an annulus $0\fdg5 < r < 1\fdg0$ is represented by the background grayscale. The blue curve shows the best-fit isochrone as described in Section 4 and Table 1. Bottom right: color–magnitude distribution of high membership probability stars.

uncertainty on the distance modulus of MagLiteS J0644−5953 (Pic II) was derived from the posterior probability distribution, marginalizing over the other parameters (most importantly the age and metallicity). There is an additional systematic uncertainty coming from the synthetic isochrone model. Fitting the data with synthetic isochrones from Dotter et al. (2008) decreased the distance modulus by 0.05 mag . This variation is consistent with the results of previous work (Drlica-Wagner et al. 2015; Koposov et al. 2015a), and we quote a systematic uncertainty on the distance modulus of ± 0.1 mag associated with the isochrone model.

Figure 2 shows the spatial and color–magnitude distribution of stellar objects surrounding MagLiteS J0644−5953 (Pic II) . To enhance contrast with the field population, we filter in color–magnitude space by selecting catalog objects within 0.1 mag of the best-fit old and metal-poor PARSEC isochrone ($\tau = 10$ Gyr, $Z = 0.0002$). The rightmost panels show the spatial and color–magnitude distributions of stars in the region color-coded with the membership probability assigned by the likelihood analysis. In addition to a densely populated main sequence, MagLiteS J0644−5953 (Pic II) has a handful of probable members on the red giant branch and a few possible horizontal branch members.

5. DISCUSSION

The low luminosity ($M_V = -3.2$) and large physical size ($r_{1/2} = 46$ pc) of MagLiteS J0644−5953 (Pic II) are consistent with the population of dark-matter-dominated Milky Way satellite galaxies (Figure 1). Specifically, MagLiteS J0644−5953 (Pic II) possesses structural properties similar to the recently confirmed dwarf galaxies Reticulum II and Horologium I (Bechtol et al. 2015; Koposov et al. 2015a). While stellar kinematic data are necessary to measure the dark matter content of MagLiteS J0644−5953 (Pic II) and assign a definitive classification, the MagLiteS photometry suggests that it will likely join the ranks of recently discovered dwarf galaxies.

The proximity between MagLiteS J0644−5953 (Pic II) and the LMC, $D_{\rm LMC} = 11.3^{+3.1}_{-0.9}$ kpc, is suggestive of a physical association between these two systems. Several studies have shown that the population of old LMC stars extends to radii >13kpc (Muñoz et al. 2006; Majewski et al. 2009; Saha et al. 2010; Balbinot et al. 2015; Mackey et al. 2016). Additionally, kinematic measurements by van der Marel & Kallivayalil (2014) suggest that the LMC tidal radius is at least 16 kpc , and may be as large as 22 ± 5 kpc, which places MagLiteS J0644−5953 (Pic II) well within the LMC sphere of influence. The most distant LMC star clusters reside at similar

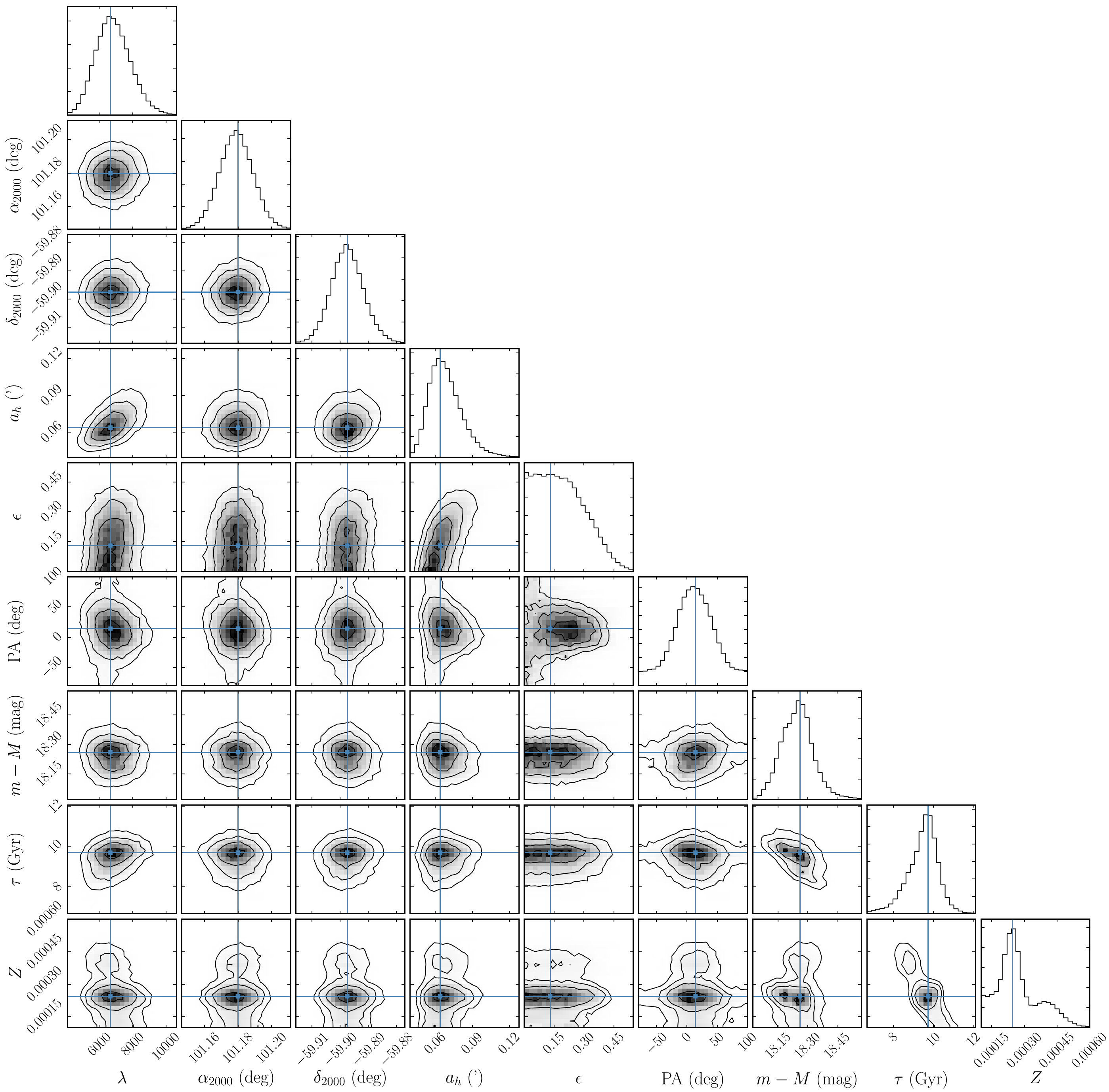

Figure 3. Posterior probability densities from a nine-parameter maximum-likelihood fit of MagLiteS J0644−5953 (Pic II) . From left to right the nine parameters are as follows: stellar richness (λ), right ascension (α_{2000}), declination (δ_{2000}), semimajor half-light radius (a_h), ellipticity (ϵ), position angle (P.A.), distance modulus ($m - M$), age (τ), and metallicity (Z). The crosshairs indicate the best-fit parameter values from a kernel density estimate of the peak of the posterior distribution.

distances: NGC 1841 at $D_{\rm LMC} = 14.9$ kpc, Reticulum at $D_{\rm LMC} = 11.4$ kpc, and ESO 121-SC03 $D_{\rm LMC} = 9.7$ kpc (Schommer et al. 1992). If MagLiteS J0644−5953 (Pic II) is bound to the LMC it would be expected to have a line-of-sight velocity that is similar to these clusters: 214 km s^{-1}, 243 km s^{-1}, and 309 km s^{-1}, respectively (Schommer et al. 1992, and references therein). Incidentally, MagLiteS J0644−5953 (Pic II) is located at a heliocentric distance that is consistent with the plane of the LMC disk (∼46 kpc; van der Marel & Kallivayalil 2014).

Several recent studies have used numerical simulations to investigate the evolution of the Magellanic system as it was accreted onto the Milky Way (i.e., Deason et al. 2015; Jethwa et al. 2016). Using the ELVIS simulations (Garrison-Kimmel et al. 2014), Deason et al. (2015) find that >40% of satellites galaxies that are currently located at $D_{\rm LMC} < 20$ kpc were bound to the LMC before infall into the Milky Way. This fraction increases to >65% if the Magellanic group was accreted recently ($\tau_{\rm infall} < 2$ Gyr) and >80% when considering only dynamical analogs of the LMC. Based on these results, if

Table 1
Observed and Derived Properties of MagLiteS J0644−5953 (Pic II)

Parameter	Value	Units
α_{2000} , δ_{2000}	101.180, −59.897	deg, deg
a_h	$3.8^{+1.5}_{-1.0}$	arcmin
r_h	$3.6^{+1.5}_{-0.9}$	arcmin
ϵ	$0.13^{+0.22}_{-0.13}$	…
P.A.	14^{+60}_{-66}	deg
$m - M$	$18.3^{+0.12}_{-0.15} \pm 0.1$ [a]	…
τ	10^{+1}_{-2}	Gyr
Z	$0.0002^{+0.0003}_{-0.0001}$	…
$\sum p_i$	153^{+12}_{-12}	…
TS	235	
$D_{\odot}$	45^{+5}_{-4}	kpc
$r_{1/2}$	46^{+15}_{-11}	pc
M_V	$-3.2^{+0.4}_{-0.5}$ [b]	mag
M_*	$1.6^{+0.5}_{-0.3}$	$10^3 M_{\odot}$
μ	28.5^{+1}_{-1}	mag arcsec^{-2}
[Fe/H]	$-1.8^{+0.3}_{-0.3}$	dex
$E(B - V)$	0.107	mag
$D_{\rm LMC}$	$11.3^{+3.1}_{-0.9}$	kpc
$D_{\rm SMC}$	35^{+3}_{-2}	kpc
$D_{\rm GC}$	45^{+5}_{-4}	kpc

Notes. Uncertainties were derived from the highest density interval containing the peak and 90% of the marginalized posterior distribution.
[a] We assume a systematic uncertainty of ±0.1 associated with isochrone modeling.
[b] The uncertainty in M_V was calculated following Martin et al. (2008) and does not include uncertainty in the distance.

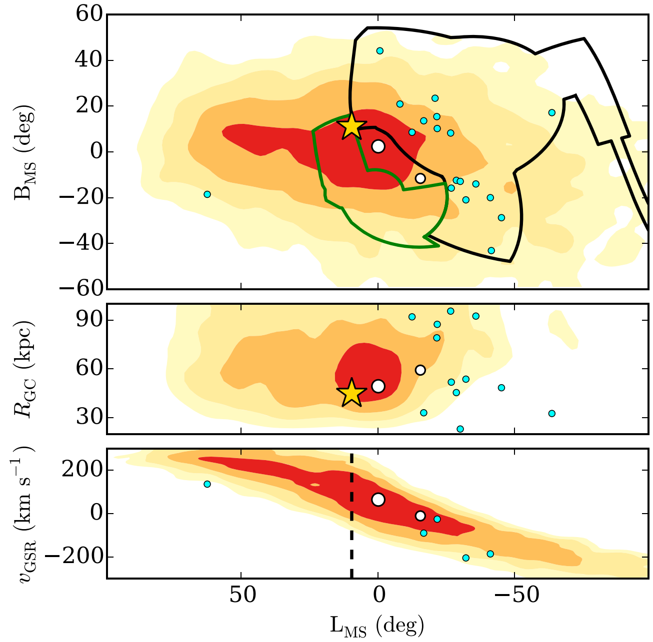

Figure 4. Phase space coordinates of MagLiteS J0644−5953 (Pic II) (gold star) relative to the simulated distribution of LMC satellites from Jethwa et al. (2016), represented by colored contours. Recently discovered DES satellites and Hydra II are shown with cyan markers. Top: the density of simulated LMC satellites projected onto the sky in MS coordinates. The DES and MagLiteS footprints are outlined in black and green, respectively. Middle: the density of simulated LMC satellites with $5° < B_{\rm MS} < 25°$ projected onto the plane of Galactocentric radius and MS longitude. Bottom: distribution of line-of-sight velocities in the Galactocentric standard reference frame for simulated satellites of the LMC. The black dashed line represents the MS longitude of MagLiteS J0644−5953 (Pic II) . The figure is adapted from Jethwa et al. (2016).

MagLiteS J0644−5953 (Pic II) originated as a member of the LMC group then it would have a radial velocity that is within ∼150 km s^{-1} of that of the LMC.

Jethwa et al. (2016) used dedicated simulations to model the dynamics of the Milky Way, LMC, and SMC, and concluded that 30% of the Milky Way's satellite galaxies originated with the LMC. They predict that satellites of the LMC are distributed within ±20° of the plane of the Magellanic Stream (MS; Nidever et al. 2008) and would be preferentially found at positive MS longitudes in a leading arm of satellites (Figure 4). The MS coordinates of MagLiteS J0644−5953 (Pic II) , $(L_{\rm MS}, B_{\rm MS}) = 9°.58, 11°.11$, lie within the preferred region for Magellanic satellites and are well-aligned with the putative plane connecting the LMC, SMC, and the DES-discovered satellites with $B_{\rm MS} < 0°$ (Jethwa et al. 2016). Furthermore, the simulations of Jethwa et al. (2016) predict that MagLiteS J0644−5953 (Pic II) has a line-of-sight velocity in the Galactic standard of rest (GSR) in the range of 15 km s^{-1} $< v_{\rm GSR} <$ 175 km s^{-1} (68% interval).

Taken together, the photometric properties of MagLiteS J0644−5953 (Pic II) and recent simulations of the Magellanic system support the hypothesis that MagLiteS J0644−5953 (Pic II) is a dwarf galaxy that arrived at the Milky Way as part of the Magellanic system. However, kinematic measurements are required to confirm the past or present relationship between MagLiteS J0644−5953 (Pic II) and its massive nearby neighbors. If MagLiteS J0644−5953 (Pic II) is confirmed to be a gravitationally bound galactic companion of the LMC, it would be the most direct example of a satellite of a satellite within the Local Group, further supporting the standard cosmological framework of hierarchical structure formation. The fortuitous discovery of MagLiteS J0644−5953 (Pic II) in early MagLiteS data will be followed by more comprehensive searches for satellite galaxies once additional data are collected.

We thank Prashin Jethwa for sharing results from his simulated model of LMC satellites.

This project used data obtained with the Dark Energy Camera (DECam), which was constructed by the DES collaboration. We gratefully acknowledge the DES data management group at NCSA for processing the images. The DES data management system is supported by the National Science Foundation under grant No. AST-1138766.

Funding for the DES Projects has been provided by the DOE and NSF (USA), MISE (Spain), STFC (UK), HEFCE (UK), NCSA (UIUC), KICP (U. Chicago), CCAPP (Ohio State), MIFPA (Texas A&M), CNPQ, FAPERJ, FINEP (Brazil), MINECO (Spain), DFG (Germany) and the collaborating institutions in the Dark Energy Survey, which are Argonne Lab, UC Santa Cruz, University of Cambridge, CIEMAT-Madrid, University of Chicago, University College London, DES-Brazil Consortium, University of Edinburgh, ETH Zürich, Fermilab, University of Illinois, *ICE* (IEEC-CSIC), IFAE Barcelona, Lawrence Berkeley Lab, LMU München and the associated Excellence Cluster universe, University of Michigan, NOAO, University of Nottingham, Ohio State

University, University of Pennsylvania, University of Portsmouth, SLAC National Lab, Stanford University, University of Sussex, and Texas A&M University.

This research was made possible through the use of the AAVSO Photometric All-Sky Survey (APASS), funded by the Robert Martin Ayers Sciences Fund.

Facility: Blanco.

REFERENCES

Balbinot, E., Santiago, B. X., Girardi, L., et al. 2015, MNRAS, 449, 1129
Bechtol, K., Drlica-Wagner, A., Balbinot, E., et al. 2015, ApJ, 807, 50
Bertin, E. 2006, in ASP Conf. Ser. 351, Astronomical Data Analysis Software and Systems XV, ed. C. Gabriel et al. (San Francisco, CA: ASP), 112
Bertin, E. 2011, in ASP Conf. Ser., Vol. 442, Astronomical Data Analysis Software and Systems XX, ed. I. N. Evans et al. (San Francisco, CA: ASP), 435
Bertin, E., & Arnouts, S. 1996, A&AS, 117, 393
Besla, G., Kallivayalil, N., Hernquist, L., et al. 2007, ApJ, 668, 949
Bressan, A., Marigo, P., Girardi, L., et al. 2012, MNRAS, 427, 127
Busha, M. T., Wechsler, R. H., Behroozi, P. S., et al. 2011, ApJ, 743, 117
Carlin, J. L., Sand, D. J., Price, P., et al. 2016, ApJL, 828, L5
Chabrier, G. 2001, ApJ, 554, 1274
D'Onghia, E., & Lake, G. 2008, ApJL, 686, L61
Deason, A. J., Wetzel, A. R., Garrison-Kimmel, S., & Belokurov, V. 2015, MNRAS, 453, 3568
Dotter, A., Chaboyer, B., Jevremović, D., et al. 2008, ApJS, 178, 89
Drlica-Wagner, A., Bechtol, K., Rykoff, E. S., et al. 2015, ApJ, 813, 109
Flaugher, B., Diehl, H. T., Honscheid, K., et al. 2015, AJ, 150, 150
Foreman-Mackey, D., Hogg, D. W., Lang, D., & Goodman, J. 2013, PASP, 125, 306
Garrison-Kimmel, S., Boylan-Kolchin, M., Bullock, J. S., & Lee, K. 2014, MNRAS, 438, 2578
Jethwa, P., Erkal, D., & Belokurov, V. 2016, MNRAS, 461, 2212
Kallivayalil, N., van der Marel, R. P., Besla, G., Anderson, J., & Alcock, C. 2013, ApJ, 764, 161
Kim, D., & Jerjen, H. 2015, ApJL, 808, L39
Koposov, S. E., Belokurov, V., Torrealba, G., & Evans, N. W. 2015a, ApJ, 805, 130
Koposov, S. E., Casey, A. R., Belokurov, V., et al. 2015b, ApJ, 811, 62
Laevens, B. P. M., Martin, N. F., Bernard, E. J., et al. 2015a, ApJ, 813, 44
Laevens, B. P. M., Martin, N. F., Ibata, R. A., et al. 2015b, ApJL, 802, L18
Lynden-Bell, D. 1976, MNRAS, 174, 695
Mackey, A. D., Koposov, S. E., Erkal, D., et al. 2016, MNRAS, 459, 239
Majewski, S. R., Nidever, D. L., Muñoz, R. R., et al. 2009, in IAU Symp. 256, The Magellanic System: Stars, Gas, and Galaxies, ed. J. T. Van Loon & J. M. Oliveira (Cambridge: Cambridge Univ. Press), 51
Martin, N. F., de Jong, J. T. A., & Rix, H.-W. 2008, ApJ, 684, 1075
Martin, N. F., Nidever, D. L., Besla, G., et al. 2015, ApJL, 804, L5
Mohr, J. J., Armstrong, R., Bertin, E., et al. 2012, Proc. SPIE, 8451, 84510D
Muñoz, R. R., Majewski, S. R., Zaggia, S., et al. 2006, ApJ, 649, 201
Nichols, M., Colless, J., Colless, M., & Bland-Hawthorn, J. 2011, ApJ, 742, 110
Nidever, D. L., Majewski, S. R., & Butler Burton, W. 2008, ApJ, 679, 432
Nidever, D. L., Majewski, S. R., Butler Burton, W., & Nigra, L. 2010, ApJ, 723, 1618
Saha, A., Olszewski, E. W., Brondel, B., et al. 2010, AJ, 140, 1719
Sales, L. V., Navarro, J. F., Cooper, A. P., et al. 2011, MNRAS, 418, 648
Sales, L. V., Navarro, J. F., Kallivayalil, N., & Frenk, C. S. 2016, MNRAS, submitted (arXiv:1605.03574)
Sand, D. J., Spekkens, K., Crnojević, D., et al. 2015, ApJL, 812, L13
Schlafly, E. F., & Finkbeiner, D. P. 2011, ApJ, 737, 103
Schlegel, D. J., Finkbeiner, D. P., & Davis, M. 1998, ApJ, 500, 525
Schommer, R. A., Suntzeff, N. B., Olszewski, E. W., & Harris, H. C. 1992, AJ, 103, 447
Sevilla, I., Armstrong, R., Bertin, E., et al. 2011, in Proc. DPF-2011 Conf., arXiv:1109.6741
Torrealba, G., Koposov, S. E., Belokurov, V., et al. 2016b, MNRAS, 463, 712
Torrealba, G., Koposov, S. E., Belokurov, V., & Irwin, M. 2016a, MNRAS, 459, 2370
Tucker, D. L., Annis, J. T., Lin, H., et al. 2007, in ASP Conf. Ser. 364, The Future of Photometric, Spectrophotometric and Polarimetric Standardization, ed. C. Sterken (San Francisco, CA: ASP), 187
van der Marel, R. P., & Kallivayalil, N. 2014, ApJ, 781, 121
Walker, M. G., Mateo, M., Olszewski, E. W., et al. 2016, ApJ, 819, 53
Wheeler, C., Oñorbe, J., Bullock, J. S., et al. 2015, MNRAS, 453, 1305
Yozin, C., & Bekki, K. 2015, MNRAS, 453, 2302
Zacharias, N., Finch, C. T., Girard, T. M., et al. 2013, AJ, 145, 44